

1 <https://doi.org/10.1007/s11707-020-0817-1>

2 Front. Earth Sci.

3 Rezuhanul ISLAM et al. Typhoon parameter sensitivity of storm surge in the semi-enclosed Tokyo Bay

4 RESEARCH ARTICLE

5 Typhoon parameter sensitivity of storm surge in the semi-enclosed 6 Tokyo Bay

7 Md. Rezuhanul ISLAM*, Hiroshi TAKAGI

8 School of Environment and Society, Tokyo Institute of Technology, Tokyo 152-8550, Japan

9 Received November 30, 2019; accepted March 5, 2020

10 E-mail: islam.m.ac@m.titech.ac.jp

11 © Higher Education Press and Springer-Verlag GmbH Germany, part of Springer Nature 2020

12 Abstract

13 In this study, a storm surge model of the semi-enclosed Tokyo Bay was constructed to investigate its hydrodynamic
14 response to major typhoon parameters, such as the point of landfall, approach angle, forward speed, size, and
15 intensity. The typhoon simulation was validated for Typhoon Lan in 2017, and 31 hypothetical storm surge scenarios
16 were generated to establish the sensitivity of peak surge height to the variation in typhoon parameters. The maximum
17 storm surge height in the upper bay adjacent to the Tokyo Metropolitan Area was found to be highly sensitive to the
18 forward speed and size of the passing typhoon. However, the importance of these parameters in disaster risk reduction
19 has been largely overlooked by researchers and disaster managers. It was also determined that of the many
20 hypothetical typhoon tracks evaluated, the slow passage of a large and intense typhoon transiting parallel to the
21 longitudinal axis of Tokyo Bay, making landfall 25 km southwest, is most likely to cause a hazardous storm surge
22 scenario in the upper-bay area. The results of this study are expected to be useful to disaster managers for advanced
23 preparation against destructive storm surges.

24 **Keywords** storm surge, risk, semi-enclosed bay, typhoon parameters, parametric study, Typhoon Lan

25 1 Introduction

26 Typhoon-induced storm surges are a considerable threat to coastal inhabitants in Japan. On average, three typhoons
27 a year make landfall on the main islands of Japan. Although the associated human losses are not extreme, with annual
28 total fatalities of less than 40 over the past decade, billions of dollars in damage is inflicted upon Japan's infrastructure
29 every year by these events (JMA, 2019a; Digital Typhoon, 2019). In particular, the Northwest Pacific typhoon
30 seasons of 2004, 2005, 2017, 2018, and 2019 were the most disastrous for Japan in recent decades with the occurrence
31 of several historic typhoons, including Chaba (2004), Nabi (2005), Lan (2017), Jebi (2018), Faxai (2019), and Hagibis
32 (2019) (Digital Typhoon, 2019). In 2004, more than 30,000 houses were flooded by storm surges induced by Typhoon
33 Chaba (2004) in western Japan's Seto Inland Sea (Higaki et al., 2009). More recently, the two prosperous economic
34 regions of Kanto and Kansai suffered their highest recorded storm surges during the passage of Typhoon Lan and
35 Typhoon Jebi, respectively (Islam et al., 2018; Le et al., 2019). In 2019, the compact but strong Typhoon Faxai
36 generated historically high waves inside Tokyo Bay, causing the destruction of nearly 400 factories in Yokohama
37 Port (Takagi et al., 2020).

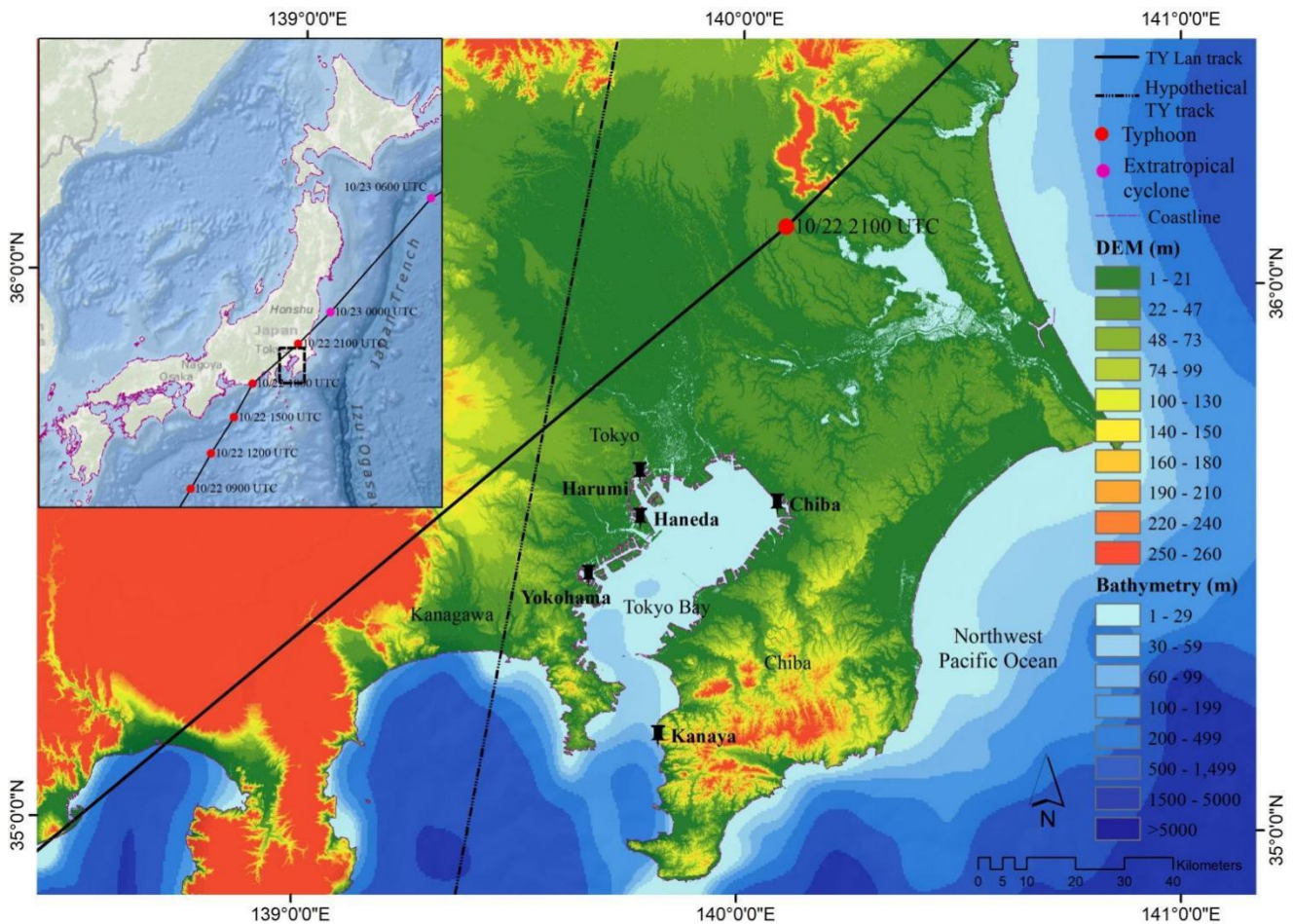
38 Precise and timely forecasts informing effective warnings are essential to mitigate the risks to life and property
39 posed by typhoons and their associated storm surges (Takagi et al., 2018; Takagi et al., 2019). The Japan
40 Meteorological Agency (JMA) has historically been responsible for monitoring and reporting weather data, in
41 addition to forecasting storm surge. The JMA uses a two-dimensional numerical model which was improved in 2007
42 by incorporating a non-hydrostatic mesoscale model. The JMA model predicts multiple storm surge scenarios using
43 different meteorological forcing fields that account for strong shoreward winds and pressure systems to consider the
44 uncertainty in typhoon track forecasts (Higaki et al., 2009). However, one of the major shortcomings of this model
45 is its inability to account for other variable typhoon parameters (e.g., size and forward speed) that have a direct
46 influence on storm surge generation (Needham and Keim, 2011). Further improvement in storm surge forecasting is
47 fundamental to reduce related loss of life and property damage. Essentially, such improvement can only be achieved
48 through an in-depth understanding of both the physical parameters and the behavior of storm surge in a particular
49 coastal region.

50 Several recent studies have attempted to use computational modeling to quantify the factors that most influence
51 storm surge behavior. For example, Irish et al. (2008) showed that storm surge tends to increase with hurricane size,
52 and concluded that hurricane approach angle could also affect surge height. Specifically, hurricanes making landfall
53 on the Gulf Coast of the United States with a more easterly heading were found to produce higher surges than those
54 with a northerly track. Regarding the effect of hurricane forward speed on storm surge, an investigation of the
55 Louisiana–Texas coasts (USA) by Rego and Li (2009) revealed that slower hurricanes (with a forward speed of 12.6–
56 18.0 km/h) cause more extensive flooding, while faster hurricanes produce higher surges but with comparatively less
57 flood volume. Zhang and Li (2019) performed an idealized numerical experiment and found that faster hurricanes
58 increase the height of storm surge as the forced storm surge waves overlap with the Kelvin wave which is not observed
59 in hurricanes with slower movement. More recently, Sebastian et al. (2014) found that storm surge behavior in a
60 small water basin, such as Galveston Bay (USA), is highly sensitive to the local wind direction associated with
61 hurricane landfall location. This finding supports Weisberg and Zheng's (2006) conclusion that the greatest storm
62 surge event would occur when a hurricane makes landfall to the north of Tampa Bay (USA), resulting in maximum
63 wind storms at the mouth of the bay. Inspired by these previous studies on the dependence of storm surge on various
64 parameters of tropical cyclones, thus increasing the understanding of storm surge climatology in the US Gulf Coast,
65 the present study examined the potential risk in Tokyo Bay, Japan.

66 The population of the Tokyo Metropolis was estimated in May 2017 at 13.7 million (MHLW, 2018). It is located
67 northwest of Tokyo Bay (35°41'N, 139°41'E), one of the most populous coastal regions in the world. The Bay (Fig.
68 1) has an intricate coastline that can either defend the megacity comprising Tokyo, Kanagawa, and Chiba Prefectures
69 against storm surge or render it particularly vulnerable because of trapping and amplification effects (Hirano et al.,
70 2014). Although Tokyo is prone to the effects of typhoons, the frequency of typhoon landfall in the region is not
71 remarkably high compared with that in southwestern Japan. Nevertheless, strong typhoons do sometimes venture
72 into the bay. Among those that directly affected Tokyo Bay over the past century was Typhoon Taisho in 1917. The
73 storm surge claimed 1,301 lives, destroyed 43,083 houses, and swept away 8,220 marine vessels (Omori, 1918).
74 Although this represents the worst typhoon-related disaster to have affected Tokyo Bay, the mechanism of this event
75 remains poorly understood. More recently, Typhoon Lan (2017), equivalent to a Category 1 hurricane at landfall,
76 caused a 1.2-m storm surge leading to the partial inundation of the inner-bay area (Islam et al., 2018).

77 The large size and fast forward speed of Typhoon Lan raised concerns over whether the urban waterfronts of Tokyo
78 and its neighboring cities are sufficiently resilient against future powerful typhoons (Islam et al., 2018). The potential
79 hazards in the Tokyo Bay area associated with the occurrence of a catastrophic typhoon have been overlooked,
80 possibly due to the infrequency of these significant disasters. A storm surge risk assessment by the Japanese
81 government, in addition to recent scientific studies on Tokyo Bay, have highlighted the dependence of storm surge
82 on wind intensity, typhoon track, and sea level rise due to climate change (MLIT, 2009; Hoshino et al., 2016; Nakajo
83 et al., 2018). However, to the best of our knowledge, the sensitivity of storm surge to the forward speed and size of
84 typhoons has not been sufficiently investigated in this region. A better understanding of how a storm surge event
85 might evolve in Tokyo Bay in response to all typhoon parameters is necessary to ensure robust emergency
86 preparedness. The present study was therefore conducted to examine the sensitivity of storm surge behavior in Tokyo

87 Bay to major typhoon parameters (i.e., landfall location, approach angle, forward speed, size, and intensity) in order
 88 to estimate the potential maximum storm surge height.



89
 90 Fig. 1 Track of Typhoon Lan (2017) as it approached the shallow coastal areas of Tokyo Bay. The black place markers indicate
 91 measurement stations used in this study (Tide: Harumi, Yokohama, Chiba, and Kanaya; Wind: Haneda). The hypothetical typhoon track
 92 is described in Section 3.5 (Japan Oceanographic Data Center, 2000; Japan Aerospace Exploration Agency, 2015; Geospatial
 93 Information Authority of Japan, 2016; JMA, 2019b).

94 2 Methodology

95 2.1 Model description and experimental design

96 In this study, a series of numerical sensitivity experiments was conducted considering Typhoon Lan (2017) as the
 97 reference typhoon. Numerical simulations were performed to elucidate the influence of storm parameters (i.e.,
 98 landfall location, approach angle, forward speed, storm size, and wind intensity) on storm surge generation in Tokyo
 99 Bay. For this purpose, a parametric typhoon model developed by Takagi et al. (2012, 2014, 2016a, 2017) was coupled
 100 with the Delft3D-FLOW fluid dynamics model (Deltares, 2011). The accuracy of this typhoon model has been
 101 validated for recent typhoons, such as Haiyan (2013) (Takagi et al., 2016a), Goni (2015) (Takagi and Wu, 2016b),
 102 Hato (2017) (Takagi et al., 2018), and Jebi (2018) (Le et al., 2019), all of which occurred in the Northwest Pacific
 103 basin. The typhoon model calculates both the pressure and wind fields using parameters obtained from the JMA best-
 104 track data set, which includes the central position of the typhoon, pressure, and 50-kt (26-m/s) wind radius (R_{50}) for
 105 each recording period. Delft3D-FLOW was then used to simulate the propagation of storm surge from the deep sea
 106 into shallow waters. Since this study used a 2D horizontal grid to model the storm surge, the code is equivalent to a
 107 nonlinear longwave model as is commonly used for storm surge studies. The simulation was performed over a wide
 108 area with a grid size of 50 m (Fig. 1) encompassing parts of Tokyo, Kanagawa, and Chiba Prefectures to assess

109 potentially affected areas. The domain incorporated both the geometries of landfills and rivers surrounding inner
 110 Tokyo Bay, where the mean bathymetry is approximately 5 m. The bathymetry data (50-m resolution) over the target
 111 area and astronomical tide data were obtained from the Japan Coast Guard and the TPXO7.1 Global Tide Model
 112 (Egbert and Erofeeva, 2002), respectively. The numerical settings used in this study are listed in [Table 1](#).

113 Typhoon Lan made landfall at 18:00 UTC on September 22, 2017, approximately 125 km southwest of Tokyo Bay
 114 (Fig. 1) with a maximum wind speed of 40 m/s (equivalent to a Category 1 on the Saffir-Simpson hurricane wind
 115 scale). It was a fast-moving typhoon with a forward speed of 65 km/h at landfall and a large wind field (a 26-m/s
 116 wind radius of 389 km) generating the highest storm tide (coinciding with rising tide) on record in Yokohama and
 117 other coastal areas (e.g., Mera in southern Chiba Prefecture) (JMA, 2019c). Five experimental groups (A–E)
 118 containing a total of 31 numerical conditions, detailed in [Table 2](#), were evaluated in this study to investigate the
 119 sensitivity of surge behavior to storm parameters. The sensitivity analyses were performed by varying one of four
 120 typhoon parameters: (A) track (approach angle and landfall location), (B) forward speed, (C) size, and (D) intensity.
 121 Observations from four tide measurement stations were chosen to characterize the hydrodynamic behavior of the
 122 bay. These stations are located in the upper bay (i.e., Harumi and Chiba), middle bay (i.e., Yokohama), and lower
 123 bay (i.e., Kanaya), as shown in Fig. 1.

124 **Table 1** Numerical model settings for typhoon and storm surge simulation

Typhoon parameters	Typhoon Lan (JMA, 2019b): approach angle 140°, forward speed 65 km/h (very fast), R_{\max} of 89 km (very large)
Typhoon model	Pressure: empirical estimation by Myers formula; Wind: gradient winds considering super-gradient wind effect (Fujii and Mitsuta, 1986)
Fluid dynamics model	Delft3D-FLOW ver. 6.02
Domain	Spherical coordinate system, grid size: 50-m mesh
Bathymetry	50-m grid spacing

125 To ascertain the relationship among typhoon approach angle (θ), landfall location, and storm surge, 21 simulations
 126 of the typhoon were performed in Group A by varying θ from 0° to 180°, shifting its landfall location from the
 127 original location of Typhoon Lan to positions 100 km to the east (approximately 25 km west of the central axis of
 128 the bay) and 150 km to the east (approximately 25 km east of the central axis of the bay), while holding all other
 129 parameters constant. In this study, the approach angle θ is defined as the angle in degrees between the coastline and
 130 typhoon track, as measured clockwise from the coastline to the right of the landfall point when facing north. To
 131 investigate the extent to which typhoon forward speed influences storm surge magnitude and considering that Lan
 132 was a fast-moving typhoon, Group B shows that the forward speed of the typhoon at landfall was reduced to 36 and
 133 18 km/h (two cases). These speeds are representative of the previous two major typhoons (Danas in 2001 and Roke
 134 in 2011) to hit Tokyo Bay (JMA, 2019b). The Group C experiments focused on the effect of the maximum wind
 135 radius (R_{\max}) used to represent the size of the strongest part of a typhoon. Because R_{\max} is not included in the JMA
 136 best-track data set (Bricker et al., 2016), we converted R_{50} data into R_{\max} using the simplified equation $R_{\max} = 0.23 \times$
 137 R_{50} (Takagi and Wu, 2016b). Consequently, R_{\max} radii in the 13–89 km range at time of landfall were derived for
 138 five previous major typhoons: 1) 13 km for Danas in 2001, 2) 26 km for Mawar in 2005, 3) 43 km for Higos in 2002,
 139 4) 55 km for Kirogi in 2000, and 5) 89 km for Lan in 2017) and were used to evaluate the corresponding storm surge
 140 sensitivity (four cases). In Group D, two wind speed cases were simulated in which the original wind speed of Lan
 141 was increased and decreased by 50%.

142

143

144

145

146

Table 2 Experimental conditions, hypothesized based on Typhoon Lan (2017) as the reference typhoon

Group	Experiment	Remarks
A	Sensitivity to typhoon track (21 cases)	Original Lan track, varied approach angle from 0° (A-1) to 180° (A-7) in 30° increments. Shifted original Lan track 100 km eastward, varied approach angle from 0° (A-8) to 180° (A-14) in 30° increments. Shifted original Lan track 150 km eastward, varied approach angle from 0° (A-15) to 180° (A-21) in 30° increments.
B	Sensitivity to typhoon forward speed (two cases)	Reduced forward speed to 36 km/h (by 45%, intermediate) (B-1) and 18 km/h (by 72%, very slow) (B-2).
C	Sensitivity to typhoon size (four cases)	Reduced R_{\max} to 55 (C-1), 43 (C-2), 26 (C-3), and 13 km (very small; C-4).
D	Sensitivity to typhoon intensity (two cases)	Decreased (D-1) and increased (D-2) original Lan intensity by 50%.
E	Estimating possible maximum storm surge height (two cases)	Landfall location: 25 km southwest of Tokyo Bay, $\theta = 100^\circ$, forward speed of 18 km/h, $R_{\max} = 89$ km, Lan intensity increased by 50% at rising (E-1) and at falling tide periods (E-2).

147

148

149

150

151

152

153

154

155

156

157

Finally, the experimental conditions with the greatest influence on storm surge generation in Tokyo Bay were accounted for in the estimation of a plausible maximum storm surge height (Group E in [Table 2](#)). The generation of a storm surge against a rising and falling tide can be considerably different because of interaction mechanisms between tidal current and storm current ([Rego and Li, 2010](#); [Marsooli and Lin, 2018](#)). To address the role of tide on peak surge generation, the estimation of plausible maximum storm surge height was carried out in two cases at both rising (Typhoon Lan landfall time) and falling tide periods. Semidiurnal tidal constituents are dominant in Tokyo Bay. Hence, Typhoon Lan landfall time was shifted to six hours earlier (12:00 UTC on September 22, 2017) to reproduce the typhoon at falling tide periods. This landfall time is representative of the passage of a storm surge against a falling tide. The estimated storm surge height was then compared to the water levels recorded during the passage of Typhoon Lan and the worst-case scenario assumed by the Japanese government (MLIT, 2009). Note that in this study, the impact of waves was neglected to focus only on storm surge and to simplify the analysis.

158

2.2 Model validation

159

160

161

162

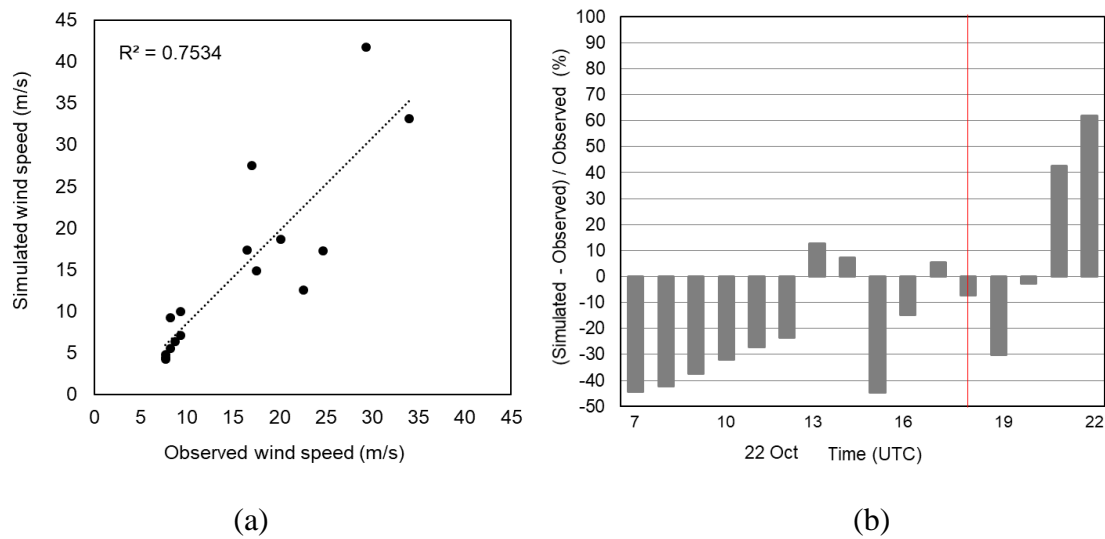
163

164

165

166

To validate the typhoon and storm surge model, simulation results, using the parameters of Typhoon Lan (2017), were compared with actual data from the observation stations collected during the typhoon's passage. A comparison of the modeled and measured wind speed ([JMA, 2019d](#)) before and after the peak storm period at the Haneda observation station is shown in [Fig. 2\(a\)](#). The coefficient of determination ($R^2 = 0.75$) indicates satisfactory agreement between the simulated and measured wind speed. However, the simulation error increased after the typhoon made landfall ([Fig. 2\(b\)](#)) as its rapid forward speed caused an abrupt change in wind speed that reduced the accuracy of the hindcast. Indeed, Typhoon Lan was a fast-moving typhoon and as such, it departed the computational domain quickly after landfall.



167

168

169

170

Fig. 2 (a) Simulated vs. observed wind speed at Haneda, Tokyo, and (b) estimated wind speed error ((simulated – observed)/observed wind speed × 100). The red vertical line indicates the time of landfall of Typhoon Lan (2017).

171

172

173

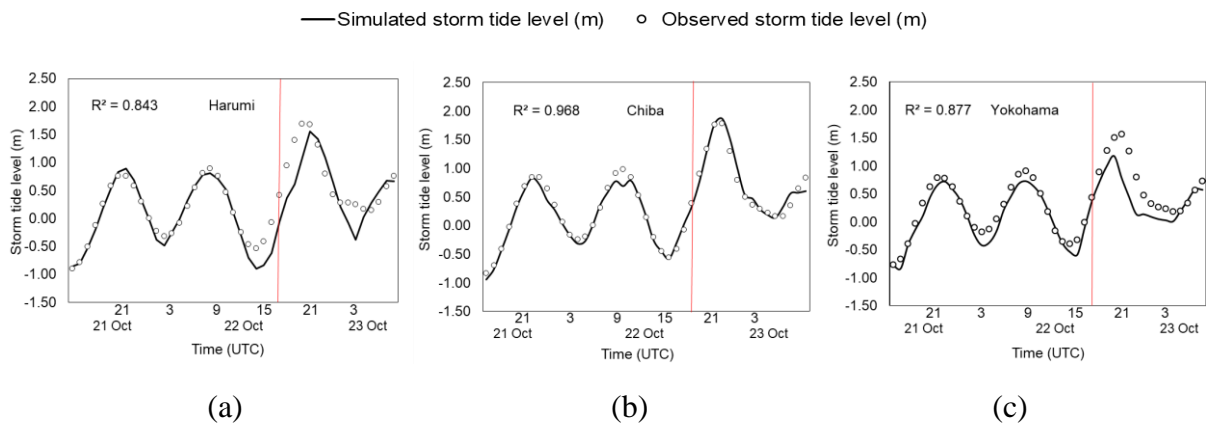
174

175

176

A comparison of the simulated and measured storm tide (JMA, 2019c) at three tide stations (Harumi, Chiba, and Yokohama) located within the computational domain is shown in Fig. 3. Model validation could not be undertaken for Kanaya because the observed storm tide data during the passage of Typhoon Lan were not available for that site. The average R^2 and root mean square errors of the three stations are 0.90 and 0.21 m, respectively. Overall, the simulated water levels agree well with the recorded tide data, although the simulated peak water levels at the Harumi and Yokohama stations are slightly underestimated.

177



178

179

180

181

Fig. 3 Comparison of observed and simulated storm tide at (a) Harumi, (b) Chiba, and (c) Yokohama. The red vertical lines indicate the time of landfall of Typhoon Lan (2017).

182 3 Results

183 3.1 Sensitivity to typhoon track (Group A)

184

185

186

187

188

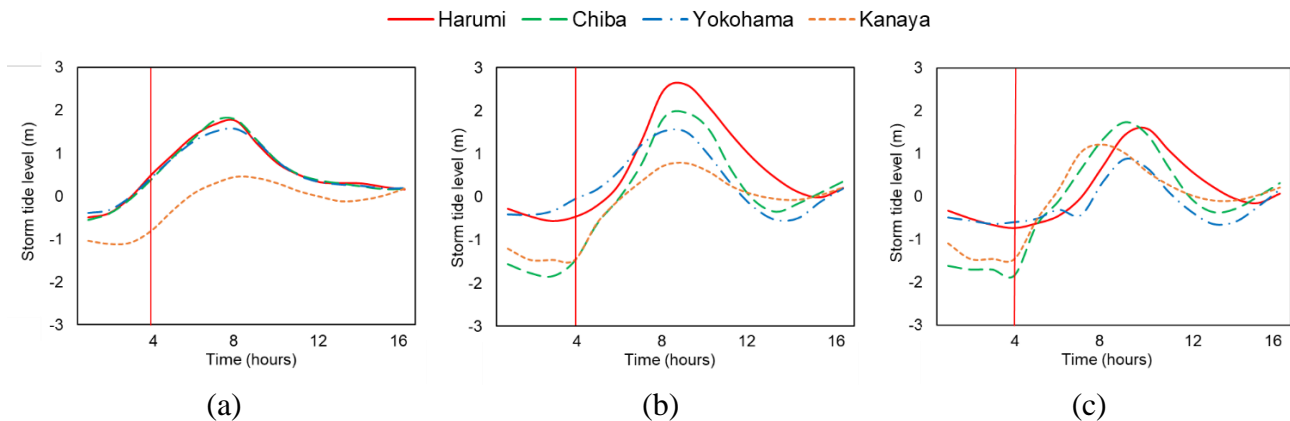
189

The simulation results indicated that typhoons traveling parallel ($90^\circ \leq \theta \leq 130^\circ$) to the axis of Tokyo Bay tended to produce higher water levels in the upper-bay area than typhoons with a more westerly ($150^\circ \leq \theta \leq 180^\circ$) or more easterly ($0^\circ \leq \theta \leq 30^\circ$) heading. In contrast, the coasts adjacent to the mouth of the bay (i.e., Kanaya) tended to be more vulnerable when typhoons traversed at a more westerly ($150^\circ \leq \theta \leq 180^\circ$) heading. Furthermore, typhoons traversing at a more easterly ($0^\circ \leq \theta \leq 30^\circ$) heading tended to cause an initial sea level drawdown of at least 1 m and dramatically steepened the storm tide profile at Yokohama. The drawdown was generated by strong, northerly

190 offshore winds that initially drove the water southward out of Tokyo Bay. Similar sea level drawdowns or negative
 191 storm surges have also been reported for the case of San Pedro Bay in the Philippines during Typhoon Haiyan in
 192 2013 which resulted in high velocity coastal flooding to heights of more than 7 m (Soria et al., 2016). The results of
 193 typhoon approach angle sensitivity tests indicate that tracks more perpendicular to the coastline to the west of Tokyo
 194 Bay tend to result in predicted peak water levels 5.5% higher on average than those produced by more oblique
 195 approach angles, particularly in the upper-bay areas (i.e., Harumi and Chiba).

196 The center of Typhoon Lan passed approximately 125 km southwest of Tokyo Bay at a θ of 140° . Figure 4(b)
 197 shows that shifting the original landfall (OL) point 100 km to the east and changing the θ to 90° (Case A-11 in Table
 198 2) increased the water level in the inner bay compared to the observed level under the original track (Fig. 4(a)).
 199 Approximately 50% of the strong southerly winds (≥ 25 m/s) blowing over the bay area due to the shift in track led

200



201

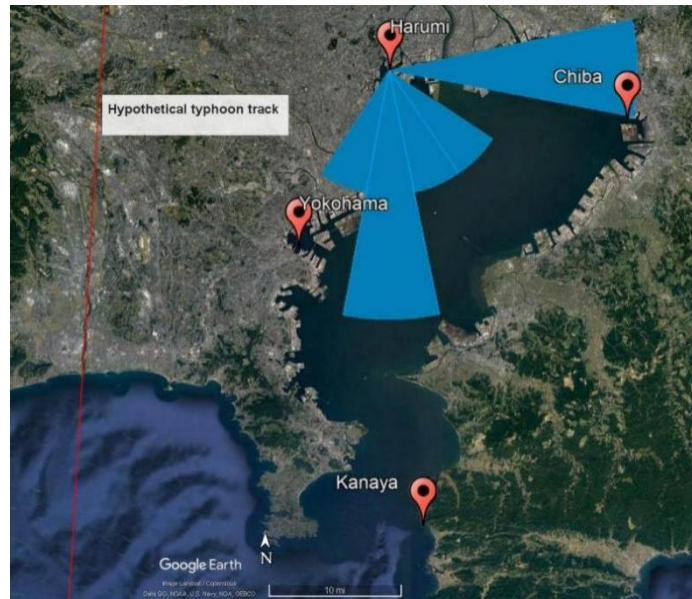
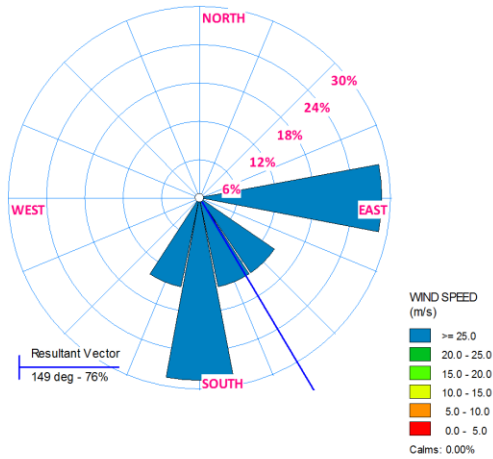
202 **Fig. 4** Comparison of storm tide level for selected sets of landfall locations and approach angles: (a) original landfall (OL; 140°
 203 approach angle), (b) 100 km east of OL and 90° approach angle (Case A-11), and (c) 150 km east of OL and 90° approach angle (Case
 204 A-18). The red vertical lines indicate time of typhoon landfall.

205 to water levels 49% higher under Case A-11 than under the OL in the innermost part of the bay (i.e., Harumi). Prior
 206 to landfall, under Case A-11, easterly winds caused a buildup of water on the west coast (Yokohama) and a draw-
 207 down in the north-eastern end of the bay (Chiba). Moreover, a large sea level gradient between the upper and lower
 208 ends of the bay was evident during the period of peak storm tide under Case A-11. For example, while the sea level
 209 at Harumi rose to over 2.5 m, the storm tide height at Kanaya changed from -1.5 to 0.8 m. A similar sea level gradient,
 210 though of a smaller magnitude, was also observed during the actual Typhoon Lan event.

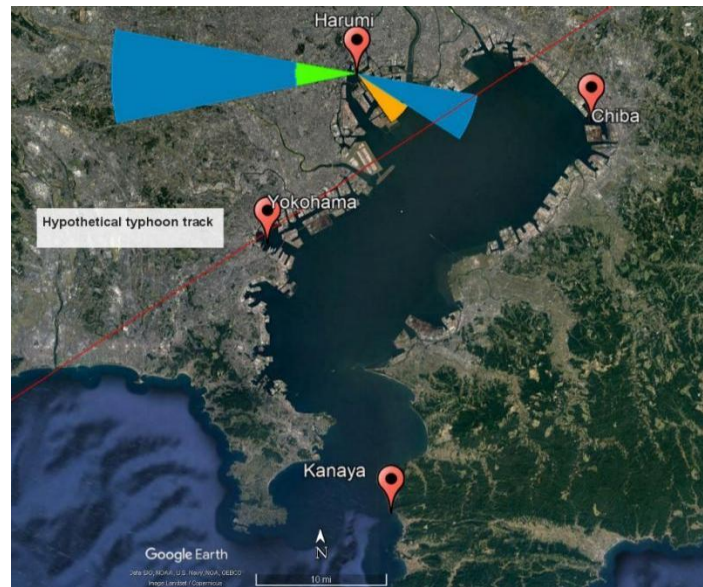
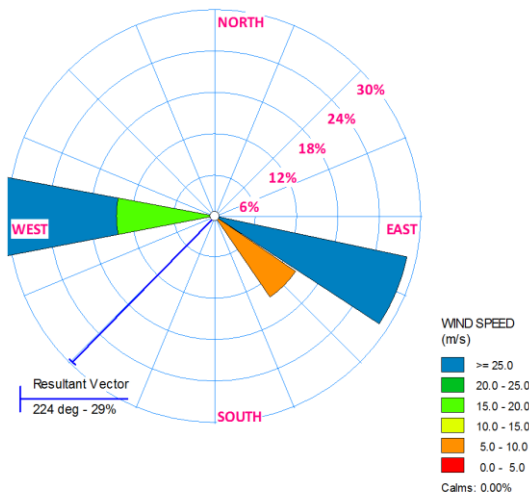
211 When the typhoon landfall was shifted 150 km to the east of the OL with an approach angle of 90° (Case A-18 in
 212 Table 2), the surface winds over the bay tended to be weaker than under the other evaluated tracks. However, as the
 213 typhoon tracked directly across the mouth of the bay (i.e., near Kanaya), the water levels increased by 0.8 m at
 214 Kanaya (Fig. 4(c)) relative to the OL (Fig. 4(a)). After the typhoon made landfall under Case A-18, strong northerly
 215 winds pushed the water out of the upper-bay area, while the destructive right-side semicircle of the typhoon covered
 216 the remainder of the bay. Indeed, the simulated peak storm tides for Case A-18 were slightly lower than for the OL
 217 at the upper-bay locations. In the middle of the bay (i.e., Yokohama), the dominant wind direction became westerly
 218 after landfall, resulting in comparatively lower water levels. The arrival of the peak storm tide in both the upper and
 219 middle parts of the bay was delayed because the strong northward wind influenced the water a few hours later than
 220 during the actual Typhoon Lan event.

221 The change in water level under different typhoon tracks confirms that the asymmetry of the wind field is highly
 222 related to the change in track. For example, the normalized frequency distribution of wind speed during landfall for
 223 Case A-11 showed that 25% of the damaging winds (≥ 25 m/s) blew directly from offshore areas to the upper bay
 224 (Fig. 5(a)); however, there was almost no damaging wind from that direction when θ was 150° (Case A-13) (Fig.
 225 5(b)). These results suggest that passage of a typhoon directly over Tokyo Bay would not necessarily correspond to

226 a more intense storm surge. However, the upper-bay areas are clearly more vulnerable to intense storm surge under
 227 a typhoon transiting parallel to Tokyo Bay 25 km southwest of its central axis.



(a)



(b)

228

229

230

231

232 **Fig. 5** Simulated wind diagram at landfall for the Harumi observation station during passage of typhoon (a) Case A-11 (landfall location
 233 25 km southwest of Tokyo Bay, $\theta = 90^\circ$); (b) Case A-13 (landfall location 25 km southwest of Tokyo Bay, $\theta = 150^\circ$).

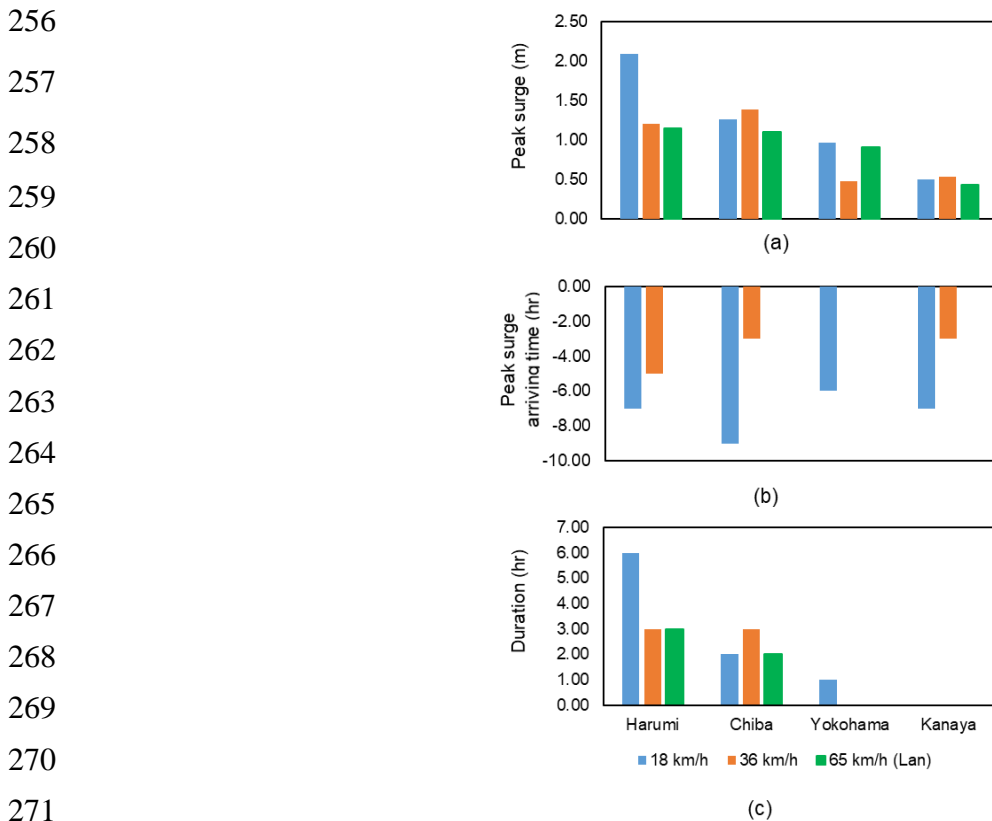
234 3.2 Sensitivity to typhoon forward speed (Group B)

235 Typhoon Lan passed southwest of Tokyo Bay with a forward speed of 65 km/h. The simulation results shown in Fig.
 236 6(a) indicate that a 45% reduction in forward speed to 36 km/h (Case B-1 in Table 2) resulted in no substantial
 237 difference in storm surge height except for Yokohama. However, a much more significant reduction in speed to 18
 238 km/h (Case B-2 in Table 2) translated into a near doubling (2.09 m) of the peak surge height in the innermost parts
 239 of the bay (i.e., Harumi), while a slight increase was evident in other places (i.e., Chiba and Yokohama). Storm surge
 240 involves the redistribution of a mass of seawater, generating a sea surface slope that depends largely on the duration

241 of axially directed wind force over the bay. For Case B-2, the typhoon took approximately 6 h to transit the bay area,
 242 whereas it took only 3 h and 2 h for Case B-1 and the actual Typhoon Lan, respectively. With this longer duration,
 243 the cross-shore components of the wind stress were able to effectively transport more water to the shallow and
 244 geometrically complex estuaries than the faster storms (Case B-1 and the actual Typhoon Lan). Consequently, a large
 245 sea level gradient in surge height developed between the upper and lower bays.

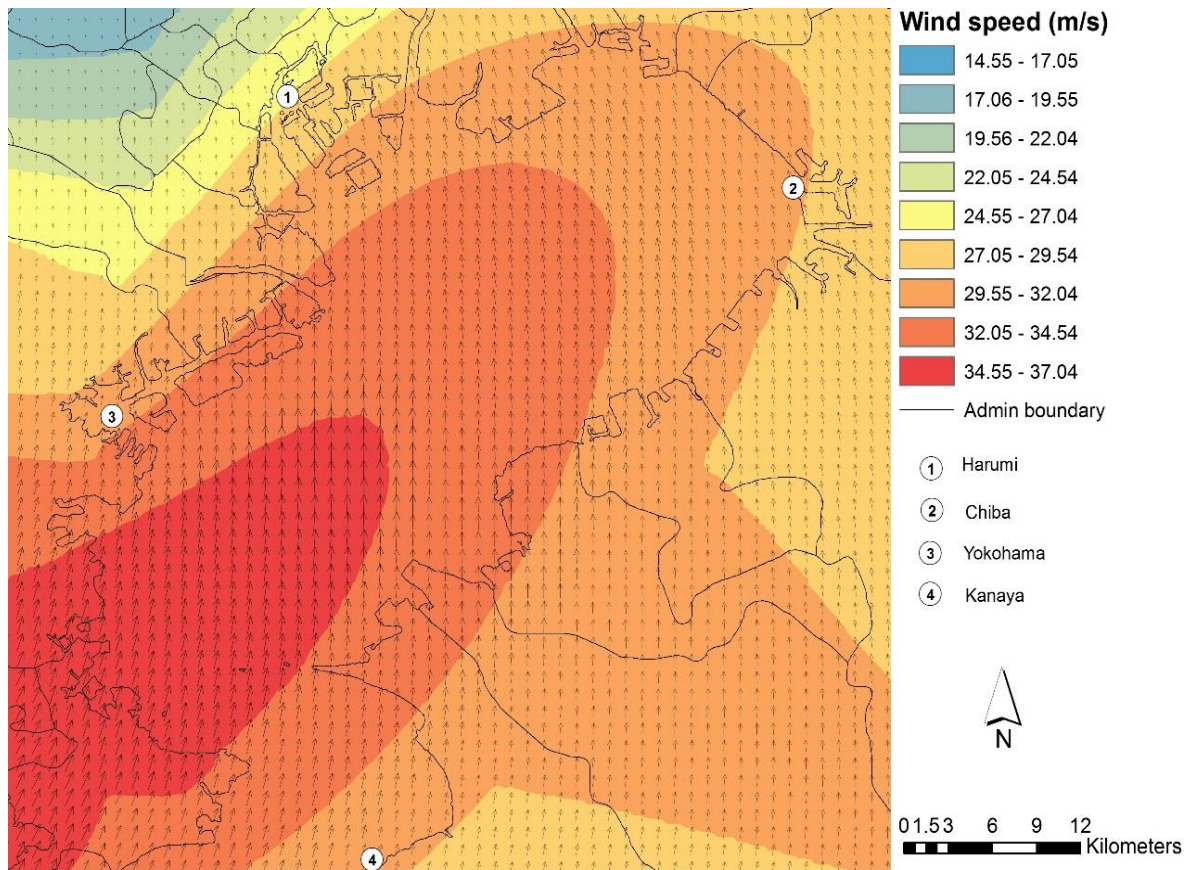
246 During peak surge, the sea levels at Harumi and Chiba were considerably different (Fig. 6(a)) because (for the
 247 given typhoon track) the dominant wind direction forced horizontal redistribution of the water mass toward the
 248 northwestern end of the bay (Fig. 7). On the east coast of the bay mouth (i.e., Kanaya), the peak surge was similar to
 249 the original observation, even though the forward speed of the typhoon was reduced (Cases B-1 and B-2). On open
 250 coasts, the effective cross-shore areas over which the winds act are smaller. Therefore, the relative decrease in
 251 typhoon wind speed with decreasing forward speed resulted in minimal change in the simulated peak surge height in
 252 these areas.

253 Figure 6(b) compares the peak surge arrival times for slower-moving typhoons relative to Typhoon Lan. Clearly,
 254 the forward speed of the typhoon strongly determines the arrival time of the maximum surge. For example, the peak
 255 surge under Case B-2 lagged behind the observed Lan peak by 7–9 h in the upper-bay area and



272 **Fig. 6** Comparison of (a) peak storm surge, (b) peak surge arrival time, and (c) duration of storm surge over 1 m for typhoons with
 273 different forward speeds. Note, the arriving times in (b) and higher surge durations in (c) are relative to those observed during the actual
 274 passage of Typhoon Lan.

275 by 6–7 h in the middle and lower bay. When the forward speed was double that of Case B-2 (i.e., Case B-1), the peak
 276 surge time still lagged behind the observed Lan peak by 3–5 h across the entire bay. In the simulations, both
 277 hypothetical typhoons Case B-1 and Case B-2 shifted the peak surge time to the low tide period, whereas Typhoon
 278 Lan caused peak surge during the high tide period (21:00 UTC, October 22, 2017) in Tokyo Bay. This finding implies
 279 that variations in typhoon forward speed could cause the peak storm surge to coincide with low/high tide periods,
 280 which should be considered in assessing storm surge risk.



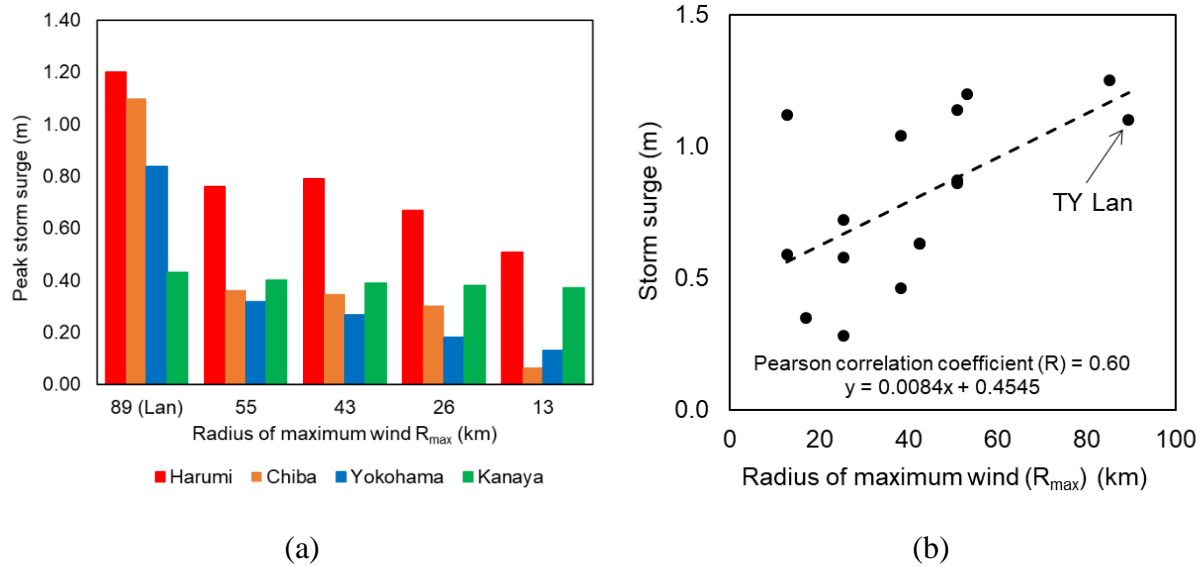
281

282 **Fig. 7** Wind speed and direction during peak surge at Harumi for typhoon forward speed of 18 km/h

283 It is apparent from Fig. 6(c) that the forward speed of the typhoon also alters the duration of the highest storm
 284 surge level (i.e., over 1 m) compared with that recorded at individual stations under Typhoon Lan. Although slowing
 285 the original forward speed to 36 km/h resulted in no substantial difference in storm surge duration, a forward speed
 286 of 18 km/h resulted in a 3-h extension of the duration of the highest storm surge level at the Harumi tidal station. In
 287 contrast, the storm surge duration at the lower-bay areas (i.e., Kanaya) remained unchanged under any typhoon speed.
 288 This is understandable because on an open coast, the buildup time is more rapid due to greater water depth, and thus
 289 the surge is less sensitive to a slow-moving typhoon. The scale of such differences between the upper and lower bay
 290 implies that the forward speed of a typhoon is an especially important parameter to consider when predicting storm
 291 surge for inner-bay locations.

292 3.3 Sensitivity to typhoon size (Group C)

293 Figure 8(a) illustrates the obtained relationship between typhoon size (in terms of R_{max}) and surge response in Tokyo
 294 Bay, indicating that storm surge height increases linearly toward the inner parts of Tokyo Bay as typhoon size (R_{max})
 295 increases. Figure 8(b) demonstrates that historical observed data support these numerical findings. Note that Chiba,
 296 Yokohama, and Kanaya are not represented in Fig. 8(b) because historical storm surge data (JMA, 2019c) relative to
 297 mean sea level (Tokyo Peil (TP)) are not available for these sites. Furthermore, the effect of typhoon size on storm
 298 surge near open coasts (i.e., Kanaya) could not be explained properly because wave-induced buildup was neglected
 299 in the numerical model: storm size affects both the fetch and the duration of generated surface waves, so wave heights
 300 tend to increase with increasing storm size, leading to higher wave buildup and greater coastal surge along open
 301 coasts (Irish et al., 2008). Nevertheless, the findings presented in Fig. 8(a) are consistent with the results of a storm
 302 surge study by Irish et al. (2008), who demonstrated that increased storm size leads to increased storm surge, a
 303 relationship that becomes more significant over areas with a flat seabed.



304

305

306

307

308

Fig. 8 (a) Comparison of peak storm surge height (in m) for typhoons of different size (in terms of R_{max}) and (b) observed peak storm surge (JMA, 2019c) vs. typhoon size (R_{max}) at typhoon landfall at the Harumi observation station during 1979–2018. The dashed line shows the correlation gradient between the observed storm surge and R_{max} .

309

310

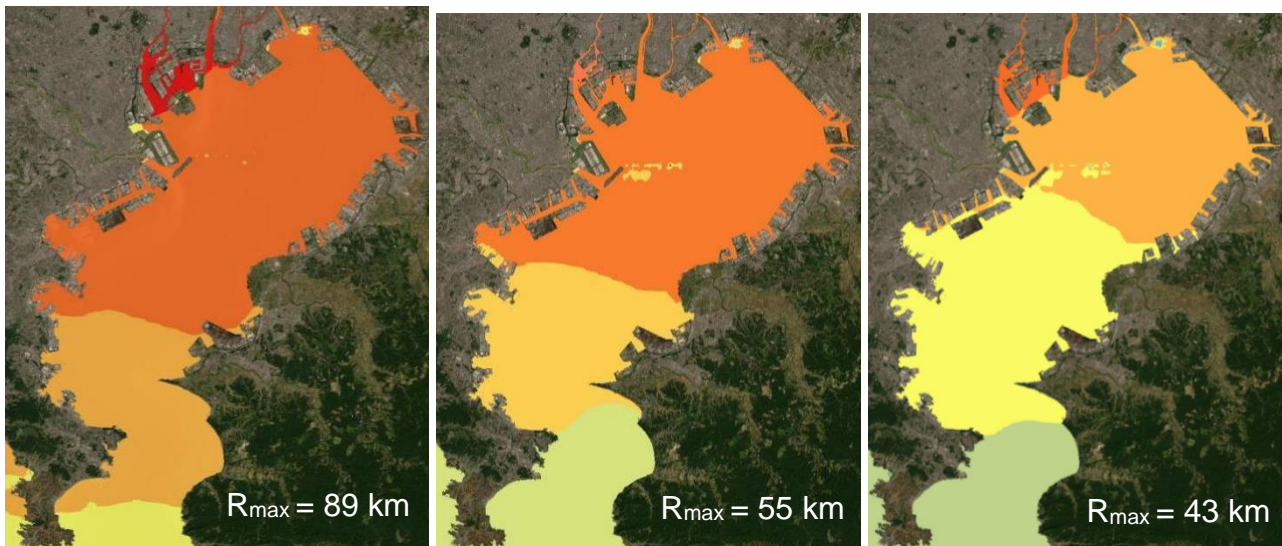
311

312

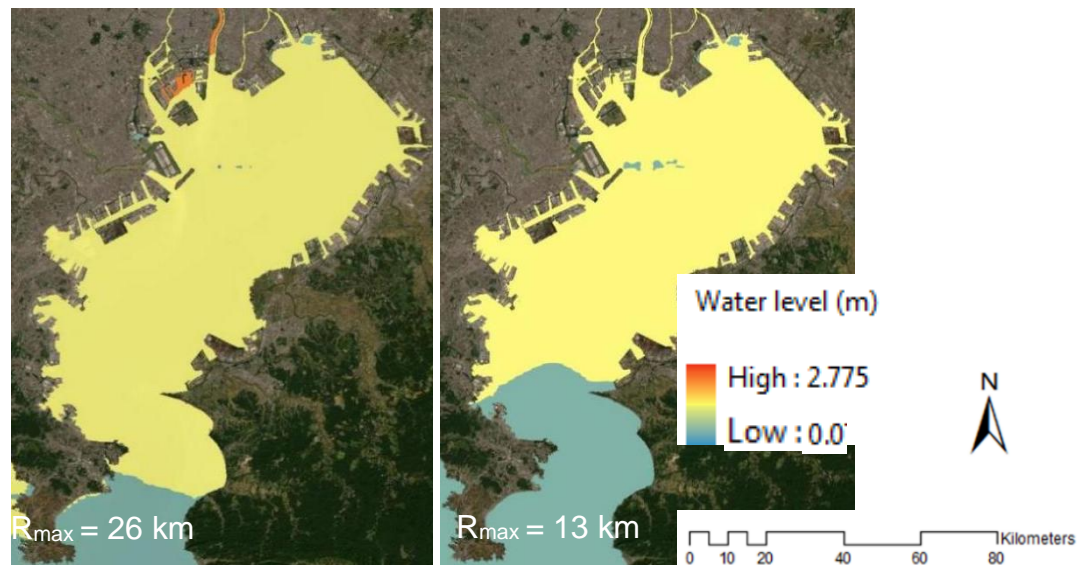
313

314

It is evident that when other typhoon parameters remain constant, the storm surge height varies with the change in typhoon size, and that this relationship is more prominent for very large typhoons. During the approach of a large typhoon, the correspondingly large swath of strong winds affects a greater sea area and induces motion in a greater quantity of water. For example, as shown in Fig. 8(a), the observed peak surge associated with Typhoon Lan ($R_{max} = 89$ km) was 34% greater than that simulated for a typhoon with $R_{max} = 43$ km (Case C-2) in the upper-bay area (i.e., Harumi).



315



316

317

Fig. 9 Distribution of simulated water level during the passage of Typhoon Lan over Tokyo Bay varying with R_{max} .

318

319

320

321

322

323

324

325

326

327

It is important to note that a certain location can be affected for a longer duration by a large typhoon than a small typhoon because it takes longer for a larger typhoon to pass. Thus, it is logical that the spatial distribution of increased water level in the upper bay would also change with typhoon size, as illustrated in Fig. 9. This finding partially explains why Typhoon Lan raised the water level by approximately 2 m in the upper areas of Tokyo Bay, even though it made landfall 125 km to the southwest. The results also show that the impact of storm surge, particularly in the inner-bay area, appears limited when a comparatively smaller typhoon (i.e., Cases C-3 and Case C-4, with $R_{max} \leq 26$ km) passes over Tokyo Bay (Fig. 8(a)). The Group C experiments thus indicate that the passage of a typhoon far from a semi-enclosed bay would not necessarily imply the occurrence of a correspondingly small storm surge. Nevertheless, upper-bay areas are shown to be more vulnerable to intense storm surge when a typhoon with a large swath of strong winds makes landfall.

328

3.4 Sensitivity to typhoon intensity (Group D)

329

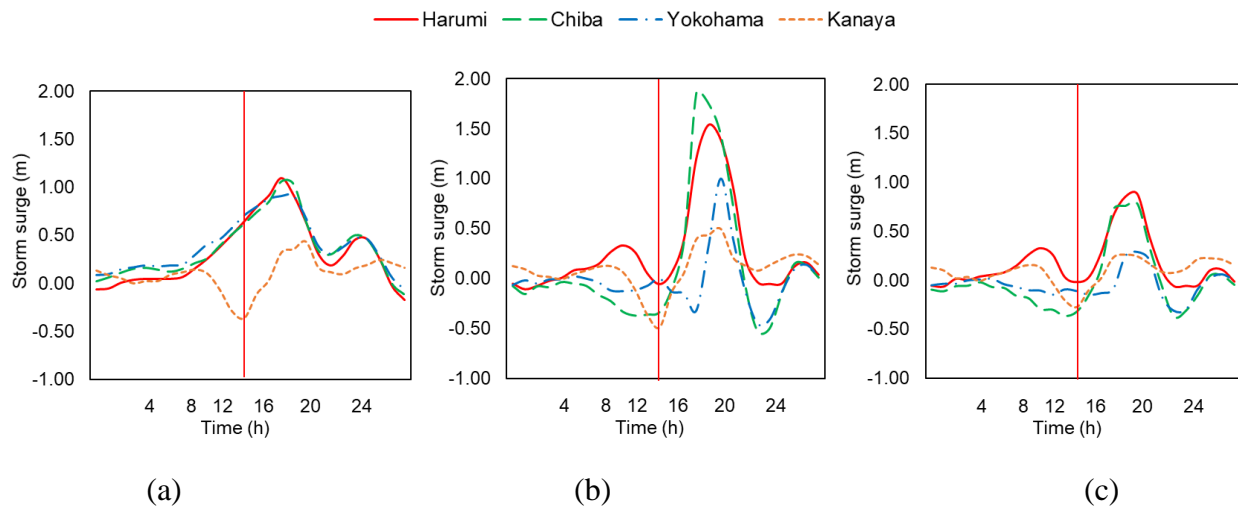
330

331

332

Figure 10 presents comparisons of observed storm surge and numerical model output for two hypothetical typhoons in which the original wind speed of Typhoon Lan was strengthened by 50% (Case D-1) and weakened by 50% (Case D-2). Increasing the intensity of Lan (Case D-1) resulted in a 40%–70% increase in storm surge height in the upper-bay area (i.e., Harumi and Chiba), whereas the increase was limited to 15% in the middle (i.e., Yokohama) and lower

333



334

335

(a)

(b)

(c)

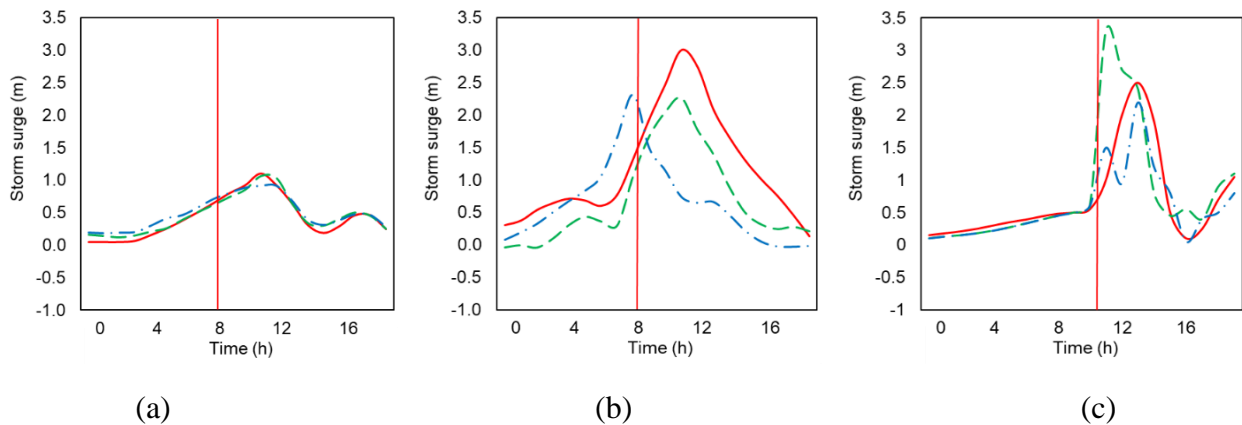
336 **Fig. 10** Storm surge hydrographs generated for (a) original Typhoon Lan, (b) 50% increase in Typhoon Lan wind speed, and (c) 50%
 337 decrease in Typhoon Lan wind speed. The red vertical lines indicate time of landfall.

338 bay areas (i.e., Kanaya). In Case D-2, although a 0.6-m difference in sea surface height existed between the upper-
 339 and lower-bay areas, a decrease in storm surge height was also evident at all stations. This sensitivity test implies
 340 that storm surge height changes exponentially in relation to surface wind speed, which is consistent with the literature
 341 (i.e. (Needham and Keim, 2013)). Furthermore, the surge hydrographs shown in Fig. 10 suggest that the arrival and
 342 recession time of the peak surge was reasonably constant within the bay system, i.e., little variation was found with
 343 the change in typhoon intensity. The shape of the surge hydrograph is more sensitive to typhoon track and forward
 344 speed, as discussed in relation to the results of the Group A and Group B experiments in Sections 3.1 and 3.2,
 345 respectively.

346 3.5 Estimating possible maximum storm surge height (Group E)

347 **Figure 11(b)** shows an example of the maximum storm surge height in Tokyo Bay determined by combining the
 348 experimental conditions found most influential in raising the water level (landfall location 25 km southwest of Tokyo
 349 Bay (Fig. 1), $\theta = 100^\circ$, forward speed of 18 km/h, $R_{\max} = 89$ km, and Typhoon Lan wind intensity increased by 50%).
 350 This case was executed in such a manner that typhoon landfall time coincided with high tide (Typhoon Lan landfall
 351 time) (Case E-1). In the innermost part of the bay (i.e., Harumi), the storm surge height increased to 3 m (storm tide:
 352 3.5 m) from 1.2 m (storm tide: 1.7 m) under Typhoon Lan, shown in Fig. 11(a), exceeding the government
 353 approximated maximum value of 2.5 m (MLIT, 2009), shown in Fig. 11 (c), by 20%. Such a variation could be
 354 explained by the differences in the experimental conditions. In the government assessment of storm surge risk, a
 355 landfall location 25 km southwest of Tokyo Bay, typhoon approach angle of approximately 100° , forward speed of
 356 50 km/h, and intensity of 915 hPa at landfall time, as well as a sea level rise of 0.6 m due to global warming, were
 357 assumed (18). However, the influence of typhoon size and speed, in this case a large and slow typhoon, was ignored
 358 when estimating the worst-case scenario for Tokyo Bay.

359 — Harumi - - Chiba - - - Yokohama



360
 361 (a) (b) (c)
 362 **Fig. 11** Comparison of storm surge heights due to (a) Typhoon Lan; (b) a hypothetical typhoon (landfall location 25 km southwest of
 363 Tokyo Bay, $\theta = 100^\circ$, forward speed of 18 km/h, $R_{\max} = 89$ km, Lan intensity increased by 50%); and (c) the hypothetical typhoon
 364 assumed by Ministry of Land, Infrastructure, Transport and Tourism (MLIT) (landfall location 25 km southwest of Tokyo Bay, $\theta =$
 365 100° , forward speed of 50 km/h, intensity of 915 hPa at landfall time, sea level rise of 0.6 m due to global warming). The red vertical
 366 lines indicate time of landfall.

367 Estimation of the possible maximum storm surge height was also carried out at the falling tide period (Case E-2).
 368 Although the peak storm surge height in the inner most part of the bay (i.e., Harumi) remained the same (2.86 m),
 369 the maximum storm tide level (2 m) decreased by 43%. Previous literature studies (Rego and Li, 2010; Marsooli and
 370 Lin, 2018) have stated that nonlinear tide-surge interactions often significantly contribute to peak storm surge.
 371 However, the present study could not confirm the role of such nonlinear behavior on storm surge generation because

372 storm wave modeling was not conducted: wave can contribute to local current, bottom stress, and wave radiation
 373 stress considerably which control the nonlinear tide-surge interaction (Song et al., 2020).

374 The comparison of the simulated time series of storm surge height at the Harumi tidal station shown in Fig. 11(b)
 375 indicates that dangerous storm surges (i.e., over 1 m above TP) rose 3 h prior to the peak and took 5 h to recede below
 376 1 m after the peak, for a total duration of 9 h. In contrast, the government assessed the dangerous storm surge as a
 377 shorter 4 h event as shown in Fig. 11(c), primarily due to the failure to account for the effects of a large and slow-
 378 moving typhoon. Even though the height variance in the peak storm surge was less at the other tidal stations than
 379 observed in the innermost part of the bay, the discrepancies would have been greater given a different set of
 380 experimental conditions. Note that the storm surge hydrograph for Kanaya is not presented in Fig. 11 because no
 381 government assessment for this site was available. This finding suggests that surge generation in a semi-enclosed bay
 382 is dependent not only on the intensity/track of a typhoon, but also on its forward speed and size, particularly in upper-
 383 bay areas.

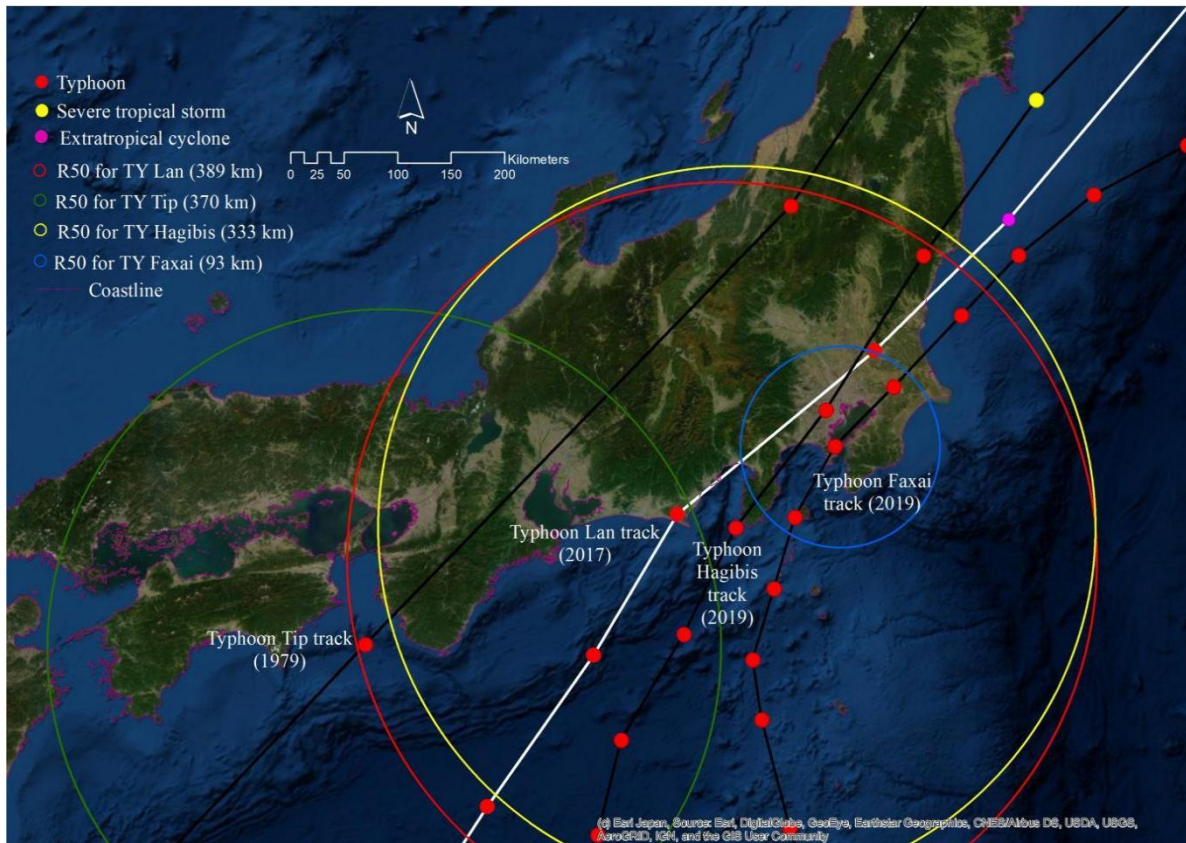
384 4 Discussion

385 Currently, the Tokyo Metropolis accounts for 10.6% of Japan's total population with a projected increase to 12.8%
 386 by 2045 (MHLW, 2018). The occurrence of typhoon-induced storm surge in Tokyo Bay could therefore not only
 387 devastate local infrastructure and cause loss of life, but also has the potential to cause unprecedented national
 388 economic and environmental damage. When predicting the risk of coastal storm surges in Tokyo Bay, wind intensity
 389 and typhoon track have traditionally been evaluated as the predominant factors. However, based on the example of
 390 Typhoon Lan, this study determined that the forward speed and size of a typhoon also exert substantial influence on
 391 the risk of coastal storm surges, particularly in the inner-most part of Tokyo Bay adjacent to the Tokyo Metropolitan
 392 Area. Findings based on numerical simulations in this study suggest that a large and slow-moving, intense typhoon
 393 transiting parallel to the longitudinal axis of Tokyo Bay on a track 25 km to the southwest is more likely to cause
 394 hazardous storm surge in the upper-bay area than a faster typhoon with less intensity. The results also indicate that
 395 the water surface elevation varies according to the intensity and track of a typhoon, consistent with current
 396 knowledge.

397 Typhoon forward speed is an oft-overlooked parameter in storm surge research. The present study has
 398 demonstrated that a slow-moving typhoon not only increases the peak storm surge height, but also affects its arrival
 399 time and duration. Although a slower typhoon could produce a greater storm surge in the bay, a fast-moving typhoon
 400 could be equally hazardous or generate a higher surge, especially on open coastlines as it would tend to coincide with
 401 the long wave propagation speed, which could energize shelf waves (Jelesnianski, 1972; Rego and Li, 2009; Thomas
 402 et al., 2019). It would appear that coastal geometry (i.e., a semi-enclosed bay or open coastline) is a critical factor in
 403 determining the relationship between storm surge and typhoon forward speed (Islam and Takagi, 2020).

404 Considering forward speed to be a function of latitude, some researchers have assumed that the forward speed of
 405 a typhoon approaching Tokyo Bay (latitude: approximately 35°N) would exceed 45 km/h (i.e., (Nakajo et al., 2018)).
 406 Based on this assumption, the government storm surge risk assessment (MLIT, 2009) neglected to consider the
 407 influence of slow-moving typhoons. However, the frequency of occurrence of slow-moving typhoons is not
 408 negligible: of the 18 typhoons that made landfall between 1961 and 2019, 5 were found to have a forward speed of
 409 less than 25 km/h at the time of landfall (JMA, 2019b). Typhoon Faxai (2019), which made landfall near Tokyo Bay
 410 (Fig. 12) at a forward speed of 24 km/h, is a recent example of this type of slow-moving typhoon. Although its
 411 intensity (Table 3) was not extreme, it still produced a historically high storm surge of 1.4 m in Chiba which remained
 412 above 1 m for 3 h (JMA, 2019c). Slow-moving Typhoon Faxai likely exited the sea state inside the bay due to its
 413 slow progression, resulting in high waves and greater storm surges that significantly damaged the port area of
 414 Yokohama. On the other hand, wind disasters were severe, resulting in damages to building roofs and collapsed
 415 power poles in various places of the Chiba prefecture. (Takagi et al., 2020). Therefore, the combined hazards from
 416 storm surge flooding, extreme winds, and prevailing vulnerabilities must be considered when developing appropriate
 417 evacuation strategies.

418 The relationship between typhoon size and storm surge height has also been underestimated partially due to limited
 419 monitoring of typhoon size by the JMA which didn't begin until 1978; thus, few examples of large typhoons such as
 420 Lan (2017) exist in the database. The variation in many of the recorded storm surges in Tokyo Bay could indeed be
 421 explained by differences in typhoon size. Typhoon Tip (1979) is a good example of a large typhoon given its R_{50}
 422 value of 370 km, four times larger than that of Typhoon Faxai (2019) ($R_{50} = 93$ km) (Fig. 12). Typhoon Tip produced
 423 a storm surge 25% (1.25 m) greater than that generated by Typhoon Faxai (1 m) in the innermost part of Tokyo Bay
 424 (i.e., Harumi) (JMA, 2019b, 2019c). Regardless of Tip's fast-moving speed (75 km/h), the maximum sustained wind
 425 speed (36 m/s) and approach angle were comparable with Faxai (Table 3). It is notable that Typhoon Tip made
 426 landfall at a much greater distance: approximately 430 km southwest of the Tokyo Bay (i.e., Minabe in Wakayama
 427 prefecture) (JMA, 2019b). However, it still managed to reach the historically highest water level of 2 m in the inner
 428 Tokyo Bay (i.e., Harumi) (JMA, 2019c). Even so, given the landfall location, the fast-moving speed may not be the
 429 major influencing factor in generating high storm surges in the case of Typhoon Tip. The greater storm surge from
 430 the larger Typhoon Tip was the result of the wider sea area affected, thus inducing motion in a greater quantity of
 431 water. The large swath of Tip's strong wind caused severe damage such that the agricultural and fishing industries
 432 sustained losses of 105.7 billion JPY (Digital Typhoon, 2019).



433

434 **Fig. 12** Tracks and 50 kt (26 m/s) wind radii (R_{50}) of Typhoon Tip (1979), Typhoon Lan (2017), Typhoon Faxai (2019), and Typhoon
 435 Hagibis (2019) during their approach to Japan (JMA, 2019b).

436 Estimation of possible maximum storm surge height based on a hypothetical typhoon has also informed several
 437 important lessons for future disaster risk management in Japan. Although the potential peak storm surge and
 438 inundation heights along Tokyo Bay are provided on the risk map edited by MLIT (2009), it remains important to
 439 evaluate the reliability of these predicted values through comparison with other hypothetical conditions. Typhoons
 440 that caused high storm surges in Tokyo Bay typically made landfall southwest (100 ± 95 km) of the central bay axis,
 441 with wind speeds of 28 to 41 m/s, an average forward speed of 46 km/h (± 19 km/h; standard deviation), and a mean
 442 R_{50} of 230 km (± 110 km; standard deviation) (Table 3). Considering historical typhoon tracks and intensities, MLIT
 443 (2009) developed a total of six scenarios (A, B, C, D, E, and F) to estimate the expected peak storm surge height. In
 444 the worst case (Scenario F), they assumed that a fast-moving typhoon (50 km/h) with a central pressure of 915 hPa

445 at the time of landfall (equivalent to the Muroto Typhoon (1934), and stronger than Typhoon Lan by 35 hPa) would
 446 travel parallel to Tokyo Bay on a track 25 km to the southwest (Fig. 1). They also assumed that owing to global
 447 warming, 0.6 m of sea level rise would have taken place so that in their present state, coastal defenses (i.e., sluice
 448 gates, breakwaters, and sea walls) would be damaged. These hypothetical typhoon conditions clearly excluded the

449 **Table 3** Top ten typhoons (1979–2009) impacting upper Tokyo Bay (i.e., Harumi) according to resultant maximum
 450 storm surge (JMA, 2019b, 2019c)

Typhoon name (Year)	Peak storm surge (m)	Landfall location from central bay axis in km (direction)	Approach angle relative to coastline (degree in clockwise direction)	Forward speed at landfall (km/h)	Radius of R_{50} at landfall (km)	Max. 10-min sustained wind speed at landfall (m/s)
Hagibis (2019)	1.38	50 (south-west)	130	37	333	41
Tip (1979)	1.25	430 (south-west)	135	75	370	36
Irma (1985)	1.20	80 (south-west)	130	69	232	33
Lan (2017)	1.20	125 (south-west)	140	65	389	41
Danas (2001)	1.12	over Tokyo Bay	120	24	56	28
Roke (2011)	1.14	190 (south-west)	140	46	222	41
Fitow (2007)	1.04	50 (south-west)	110	23	167	33
Faxai (2019)	1.01	over Tokyo Bay	135	24	93	41
Melor (2009)	0.87	250 (south-west)	145	58	222	36
Jelawat (2012)	0.86	230 (south-west)	130	50	222	36

451 combined effects of a large and slow-moving typhoon when estimating the possible maximum coastal surge in the
 452 governmental assessment. In this regard, it would be beneficial to re-evaluate the storm surge risk potentials for not
 453 only Tokyo Bay, but perhaps for other areas where the combined influence of size and forward speed, along with
 454 other parameters, have not yet been considered. The hazardous typhoon conditions addressed in Section 3.5 of this
 455 study are only hypothetical. However, the recent Typhoon Hagibis (2019) (Fig. 12) may be considered a close
 456 approximation (Table 3) of the hypothetical case.

457 In addition to its relatively slow-moving speed (37 km/h), compared to the historical average (46 km/h), Hagibis
 458 was categorized as a large ($R_{50} = 333$ km) and strong (10-min sustained wind speed of 41 m/s) typhoon. It made
 459 landfall 50 km southwest of Tokyo Bay, and had the highest storm surge in recorded history at 1.38 m (JMA, 2019b,
 460 2019c). Assuming that typhoon parameters can be independent of each other, it is unlikely, yet conceivable, that any
 461 given slow-moving typhoon transiting parallel on a track 25 km southwest of Tokyo Bay could also, simultaneously,
 462 be large and strong. Such an unusual typhoon condition clearly demonstrates its importance as an extremely
 463 hazardous scenario, similar to other conventionally evaluated worst cases (i.e., the storm surge risk assessment criteria
 464 assumed by MLIT).

465 5 Conclusions

466 For decades, typhoon disaster management in Japan has emphasized wind intensity and typhoon track to be the most
 467 dominant factors when predicting and issuing warnings for dangerous coastal storm surges. However, their
 468 forecasting techniques have not adequately accounted for the importance of other typhoon parameters to date.
 469 Considering the growing concern regarding the potential for unprecedented storm surges in the present-day Tokyo
 470 metropolitan region, this study determined the most influential typhoon parameters in storm surge generation. The
 471 results obtained suggest that incorporation of typhoon forward speed and size could help meteorologists and
 472 oceanographers provide more robust surge forecasts.

473 The sensitivity analyses presented in this paper demonstrate variations in storm surge heights related to principal
 474 typhoon parameters, including landfall location, approach angle, forward speed, size, and intensity, focused on Tokyo
 475 Bay; however, variations in typhoon parameters could also influence the generation of wind waves, which was not
 476 addressed in this study. Further research in this area should therefore examine the combined effects of wave setup,
 477 as these factors can also influence storm surge distribution. The results of the present study are based on only one
 478 historical case (Typhoon Lan). To better support future emergency planning and risk management in the vicinity of
 479 Tokyo Bay, an extension from the current scenario-based study to a probabilistic hazard assessment study is
 480 necessary.

481 Acknowledgments

482 The first author is thankful to the Ministry of Education, Culture, Sports, Science, and Technology (MEXT) of
 483 Japan for the provided scholarship to conduct research in the field of disaster risk reduction. This research was
 484 funded through the grants for Tokyo Institute of Technology (Japan Society for the Promotion of Science,
 485 16KK0121, 19K04964, and 19K24677). Best track data for 1961–2019 (www.jma.go.jp/jma/jma-eng/jma-center/rsmc-hp-pub-eg/trackarchives.html),
 486 observed tide (www.data.jma.go.jp/kaiyou/db/tide/genbo/index.php),
 487 typhoon statistics (www.data.jma.go.jp/fcd/yoho/typhoon/statistics/index.html) and past weather
 488 (www.data.jma.go.jp/obd/stats/etrn/index.php) data were provided by the Japan Meteorological Agency. No
 489 potential conflict of interest was reported by the author(s).

490 References

- 491 [Bricker J D, Roeber V, Tanaka H \(2016\)](#). Storm Surge Protection by Tsunami Seawalls in Sendai, Japan. In: *Proceedings of 35th*
 492 *International Conference on Coastal Engineering, Antalya, Turkey*. <https://doi.org/10.9753/icce.v35.management.2>
- 493 [Deltares \(2011\)](#). Delft3D-FLOW – Simulation of Multi- Dimensional Hydrodynamic Flows and Transport Phenomena, Including Sediments.
 494 User Manual Delft3DFLOW, The Netherlands, 690.
- 495 [Digital Typhoon \(2019\)](#). Typhoon Damage List.(Available at [http://agora.ex.nii.ac.jp/cgi-](http://agora.ex.nii.ac.jp/cgi-bin/dt/disaster.pl?lang=en&basin=wnp&sort=damage&order=dec&stype=number)
 496 [bin/dt/disaster.pl?lang=en&basin=wnp&sort=damage&order=dec&stype=number](http://agora.ex.nii.ac.jp/cgi-bin/dt/disaster.pl?lang=en&basin=wnp&sort=damage&order=dec&stype=number))
- 497 [Egbert G D, Erofeeva S Y \(2002\)](#). Efficient inverse modeling of barotropic ocean tides. *J Atmos Ocean Technol*, **19**(2): 183–204
 498 [doi:10.1175/1520-0426\(2002\)019<0183:EIMOBO>2.0.CO;2](https://doi.org/10.1175/1520-0426(2002)019<0183:EIMOBO>2.0.CO;2)
- 499 [Fujii T, Mitsuta Y \(1986\)](#). Synthesis of a stochastic typhoon model and simulation of typhoon winds. In: *Disaster Prevention Research*
 500 *Institute Annuals*, 29, B-1, 229–239. <https://repository.kulib.kyoto-u.ac.jp/dspace/bitstream/2433/71910/1/a29b1p22.pdf> (In Japanese)
- 501 [Geospatial Information Authority of Japan \(2016\)](#). GSI Japan Global map site. (Available at
 502 https://www.gsi.go.jp/kankyochiri/gm_japan_e.html.)
- 503 [Higaki M, Hironori H, Nozaki, F \(2009\)](#) *Outline of the Storm Surge Prediction Model at the Japan Meteorological Agency*. In: *The Technical*
 504 *Review - RSMC Tokyo-Typhoon Center*, 25 – 38. <https://www.jma.go.jp/jma/jma-eng/jma-center/rsmc-hp-pub-eg/techrev/text11-3.pdf>
- 505 [Hirano K, Bunya S, Murakami T, Iizuka S, Nakatani T, Shimokawa S, Kawasaki K \(2014\)](#). Prediction of typhoon storm surge flood in Tokyo
 506 Bay using unstructured model ADCIRC under global warming scenario. In: *Proceedings of 4th Joint US-European Fluids Engineering*
 507 *Division Summer Meeting and 12th International Conference on Nanochannels, Microchannels, and Minichannels*. Chicago, Illinois, USA:
 508 ASME.
- 509 [Hoshino S, Esteban M, Mikami T, Takagi H, Shibayama T \(2016\)](#). Estimation of increase in storm surge damage due to climate change and
 510 sea level rise in the Greater Tokyo area. *Nat Hazards*, **80**(1): 539–565 [doi:10.1007/s11069-015-1983-4](https://doi.org/10.1007/s11069-015-1983-4)
- 511 [Irish J L, Resio D T, Ratcliff J J \(2008\)](#). The influence of storm size on hurricane surge. *J Phys Oceanogr*, **38**(9): 2003–2013
 512 [doi:10.1175/2008JPO3727.1](https://doi.org/10.1175/2008JPO3727.1)
- 513 [Islam M R, Takagi H, Anh L T, Takahashi A, Bowei K \(2018\)](#). 2017 Typhoon Lan reconnaissance field survey in coasts of Kanto Region,
 514 Japan. *Journal of Japan Society of Civil Engineers, Ser. B3*. *Ocean Eng*, **74**(2) [doi:10.2208/jscejoe.74.I_593](https://doi.org/10.2208/jscejoe.74.I_593)
- 515 [Islam M R, Takagi H \(2020\)](#). Statistical significance of tropical cyclone forward speed on storm surge generation: retrospective analysis of
 516 best track and tidal data in Japan. *Georisk. Assessment and Management of Risk for Engineered Systems and Geohazards*,
 517 [doi:10.1080/17499518.2020.1756345](https://doi.org/10.1080/17499518.2020.1756345)
- 518 [Japan Aerospace Exploration Agency \(2015\)](#). 30 m World Elevation Data Site. (Available at
 519 <https://www.eorc.jaxa.jp/ALOS/en/aw3d30/data/index.htm>.)

- 520 Japan Meteorological Agency (2019a). Typhoon statistics (in Japanese). (Available at
 521 <https://www.data.jma.go.jp/fcd/yoho/typhoon/statistics/index.html>)
- 522 Japan Meteorological Agency (2019b). Typhoon Best Track Data Site. (Available at [https://www.jma.go.jp/jma/jma-eng/jma-center/rsmc-hp-](https://www.jma.go.jp/jma/jma-eng/jma-center/rsmc-hp-pub-eg/trackarchives.html)
 523 [pub-eg/trackarchives.html](https://www.jma.go.jp/jma/jma-eng/jma-center/rsmc-hp-pub-eg/trackarchives.html))
- 524 Japan Meteorological Agency (2019c). Tidal Observation Data Site (in Japanese). (Available at
 525 <http://www.data.jma.go.jp/kaiyou/db/tide/genbo/index.php>)
- 526 Japan Meteorological Agency (2019d). Past weather data (in Japanese). (Available at <http://www.data.jma.go.jp/obd/stats/etrn/index.php>)
- 527 Japan Oceanographic Data Center (2000). 500 m Gridded Bathymetric Feature Data around Japan. (Available at
 528 https://jdoss1.jodc.go.jp/vp/depth500_file.html.)
- 529 Jelesnianski C P (1972). SPLASH (Special Program to List Amplitudes of Surges from Hurricanes): 1. Landfall storms. In *NOAA Technical*
 530 *Memorandum NWS TDL-46*. Silver Spring, MD: NOAA.
- 531 Le T A, Takagi H, Heidarzadeh M, Takata Y, Takahashi A (2019). Field surveys and numerical simulation of the 2018 Typhoon Jebi: impact
 532 of high waves and storm surge in semi-enclosed Osaka Bay, Japan. *Pure Appl Geophys*, 176(10): 4139–4160 doi:10.1007/s00024-019-02295-
 533 0
- 534 Marsooli R, Lin N (2018). Numerical modeling of historical storm tides and waves and their interactions along the U.S. East and Gulf coasts. *J*
 535 *Geophys Res Oceans*, 123(5): 3844–3874 doi:10.1029/2017JC013434
- 536 Ministry of Health Labour and Welfare (Japan) (2018). Statistics and other data. (Available at
 537 <https://www.mhlw.go.jp/english/database/index.html>)
- 538 Ministry of Land Infrastructure and Transport (Japan) (2009). Estimation of large scale inundation scenario by storm surge at Tokyo Bay (in
 539 Japanese). (Available at http://www.mlit.go.jp/report/press/port07_hh_000017.html.)
- 540 Nakajo S, Fujiki H, Kim S, Mori N (2018). Sensitivity of tropical cyclone track to assessment of severe storm surge event at tokyo bay. In:
 541 *Proceedings of 36th International Conference on Coastal Engineering, Baltimore, Maryland, USA*. <https://doi.org/10.9753/icce.v36.papers.5>.
- 542 Needham H F, Keim B D (2011). Storm surge: Physical processes and an impact scale. In: Lupo E, ed. *Recent Hurricane Research—Climate,*
 543 *Dynamics, and Societal Impacts*. Croatia: Intech Open Access, 386 – 394
- 544 Needham H F, Keim B D (2013). Correlating storm surge heights with tropical cyclone winds at and before landfall. *Earth Interact*. 18: 1–26
 545 doi:10.1175/2013EI000527.1
- 546 Omori F (1918). Tsunami in Tokyo Bay. In: *Earthquake Investigation Committee Report*, 89, 19 – 48 (in Japanese).
- 547 Rego J L, Li C (2009). On the importance of the forward speed of hurricanes in storm surge forecasting: a numerical study. *Geophys Res Lett*,
 548 36(7): L07609 doi:10.1029/2008GL036953
- 549 Rego J L, Li C (2010). Nonlinear terms in storm surge predictions: Effects of tide and shelf geometry with case study from Hurricane Rita. *J*
 550 *Geophys Res*, 115(C6): 1–19 doi:10.1029/2009JC005285
- 551 Sebastian A G, Proft J M, Dietrich J C, Du W, Bedient P B, Dawson C N (2014). Characterizing hurricane storm surge behavior in Galveston
 552 Bay using the SWAN + ADCIRC model. *Coast Eng*, 88: 171–181 doi:10.1016/j.coastaleng.2014.03.002
- 553 Song H, Kuang C, Gu J, Zou Q, Liang H, Sun X, Ma Z (2020). Nonlinear tide-surge-wave interaction at a shallow coast with large scale
 554 sequential harbor constructions. *Estuar Coast Shelf Sci*, 233: 1–15 doi:10.1016/j.ecss.2019.106543
- 555 Soria J L A, Switzer A D, Villanoy C L, Fritz H M, Bilgera P H T, Cabrera O C, Siringan F P, Maria Y Y S, Ramos R D, Fernandez I Q
 556 (2016). Repeat storm surge disasters of Typhoon Haiyan and its 1897 predecessor in the Philippines. *Bull Am Meteorol Soc*, 97(1): 31–48
 557 doi:10.1175/BAMS-D-14-00245.1
- 558 Takagi H, Thao N D, Esteban M, Tam T T, Knaepen H L, Mikami T (2012). Assessment of the coastal disaster risks in Southern Vietnam.
 559 *Journal of Japan Society of Civil Engineering, B3. Ocean Eng*, 68(2): 888–893 doi:10.2208/jscejoe.68.I_888
- 560 Takagi H, Thao N D, Esteban M (2014). Tropical cyclones and storm surges in Southern Vietnam. In: Thao N D, Takagi H, Esteban M, eds.
 561 *Coastal Disasters and Climate Change in Vietnam*. Elsevier: 3 – 16. <http://dx.doi.org/10.1016/B978-0-12-800007-6.00001-0>.
- 562 Takagi H, Li S, de Leon M, Esteban M, Mikami T, Matsumaru R, Shibayama T, Nakamura R (2016a). Storm surge and evacuation in urban
 563 areas during the peak of a storm. *Coast Eng*, 108: 1–9 doi:10.1016/j.coastaleng.2015.11.002
- 564 Takagi H, Wu W (2016b). Maximum wind radius estimated by the 50 kt radius: improvement of storm surge forecasting over the Western
 565 North Pacific. *Nat Hazards Earth Syst Sci*, 16(3): 705–717 doi:10.5194/nhess-16-705-2016

Manuscript Accepted for publication in Frontiers of Earth Science
[For citing purpose - use the doi as: <https://doi.org/10.1007/s11707-020-0817-1>]

- 566 Takagi H, Esteban M, Shibayama T, Mikami T, Matsumaru R, De Leon M, Thao N D, Oyama T, Nakamura R (2017). Track analysis,
567 simulation and field survey of the 2013 Typhoon Haiyan storm surge. *J Flood Risk Manag*, 10(1): 42–52 [doi:10.1111/jfr3.12136](https://doi.org/10.1111/jfr3.12136)
- 568 Takagi H, Xiong Y, Furukawa F (2018). Track analysis and storm surge investigation of 2017 Typhoon Hato: were the warning signals issued
569 in Macau and Hong Kong timed appropriately? *Georisk. Assessment and Management of Risk for Engineered Systems and Geohazards*, 12(4):
570 297–307
- 571 Takagi H, Xiong Y, Fan J (2019). *Public Perception of Typhoon Signals and Response in Macau: Did Disaster Response Improve between the*
572 *2017 Hato and 2018 Mangkhut*. *Georisk: Assessment and Management of Risk for Engineered Systems and Geohazards*.
573 <https://doi.org/10.1080/17499518.2019.1676453>
- 574 Takagi H, Islam M R, Anh L T, Takahashi A, Sugi T, Furukawa F (2020). Investigation of high wave damage caused by 2019 Typhoon Faxai
575 in Kanto region and wave hindcast in Tokyo Bay. *Journal of Japan Society of Civil Engineers, Ser. B3. Ocean Eng*, 76(1)
576 [doi:10.2208/jscejo.76.1_12](https://doi.org/10.2208/jscejo.76.1_12)
- 577 Thomas A, Dietrich J C, Asher T G, Bell M, Blanton B O, Copeland J H, Cox A T, Dawson C N, Fleming J G, Luettich R A (2019). Influence
578 of storm timing and forward speed on tides and storm surge during Hurricane Matthew. *Ocean Model*, 137: 1–19
579 [doi:10.1016/j.ocemod.2019.03.004](https://doi.org/10.1016/j.ocemod.2019.03.004)
- 580 Weisberg R H, Zheng L (2006). Hurricane storm surge simulations for Tampa Bay. *Estuaries Coasts*, 29(6): 899–913
581 [doi:10.1007/BF02798649](https://doi.org/10.1007/BF02798649)
- 582 Zhang C, Li C (2019). Effects of hurricane forward speed and approach angle on storm surges: an idealized numerical experiment. *Acta*
583 *Oceanol Sin*, 38(7): 48–56 [doi:10.1007/s13131-018-1081-z](https://doi.org/10.1007/s13131-018-1081-z)